Journal of Physical Science and Application 4 (8) (2014) 475-483
doi: 10.17265/2159-5348/2014.08.001

Patterning of Poly(3,4-Ethylenedioxythiophene): Poly(Styrenesulfonate) Films via the Rubbing Method in Organic Photovoltaic Cells

Li-Chen Huang[1], Hung-Wei Liu[2], Tsu-Ruey Chou[1], Jung Hsieh[3], Wen-Yen Chiu[4], Leeyih Wang[2, 5] and Chih-Yu Chao[1, 3]

1. Department of Physics, National Taiwan University, Taipei 10617, Taiwan

2. Institute of Polymer Science and Engineering, National Taiwan University, Taipei 10617, Taiwan

3. Institute of Applied Physics, National Taiwan University, Taipei 10617, Taiwan

4. Department of Chemical Engineering, National Taiwan University, Taipei 10617, Taiwan

5. Center for Condensed Matter Sciences, National Taiwan University, Taipei 10617, Taiwan

Received: August 02, 2014 / Accepted: August 13, 2014 / Published: August 15, 2014.

Abstract: OPV (Organic photovoltaic) cells represent a compelling candidate for renewable energy by solar energy conversion. In recent years, versatile light-trapping measures via structures have been intensively explored to optimize photovoltaic performance. In this work, a unique rubbing technique is demonstrated to create nanoscale grooves on the PEDOT:PSS [poly(3,4-ethylenedioxythiophene): poly(styrenesulfonate)] surface and the grating-like features are 500 nm wide and 10 nm deep. The PEDOT:PSS film with grooved surface is used as buffer layers for OPV cell devices based on a P3HT:PCBM bulk heterojunction. The patterned surface has a profound effect on carrier mobility, light trapping, and hole collection efficiency, leading to an increase in the short circuit density, filling factor, and power conversion efficiency. These results indicate the feasibility of the rubbing method can be applicable to high-efficiency OPV cells.

Key words: Rubbing technique, grooved surface, organic photovoltaic cells, bulk heterojunction solar cells.

1. Introduction

OPV (Organic photovoltaic) cells have been fleetly developed in the past years since the solar energy is one of the most abundant sources in the earth and could be regarded as a prevailing technology to convert sunlight into electricity [1]. In particular, it provides relatively inexpensive materials and simple solution processable substitutes to inorganic-based photovoltaic devices [2]. In addition, the advantages of using solar cell devices over organic systems are mechanical flexibility, light weight, and can be using roll-to-roll manufacturing method at low temperatures. One of the most representative polymer solar cells is the device based on a blend of P3HT [poly (3-hexylthiophene)] as an electron donor and a soluble C_{60} derivative, PCBM (6,6-phenyl-C61-butyric acid methyl ester) as an electron acceptor. Although the PCE (power conversion efficiency) of the conventional BHJ (bulk-heterojunction) solar cell architecture consisting of P3HT:PCBM blends has reached 4%~6% by a variety of processes [3-5], its performance is still restrained by a relatively poor carrier transfer property, which has also impeded the path toward commercialization. Many studies have demonstrated that appropriate conjugated conducting polymers are attractive alternatives for applications in organic

Corresponding authors: Chih-Yu Chao and Leeyih Wang, professor, research fields: liquid crystals, structure biology and solid state lighting. E-mail: cychao@ntu.edu.tw.

electronic devices in order to obtain a high-efficiency performance [6, 7]. Accordingly, one of the commonly used semiconductive conjugated polymers is poly (3,4-ethylenedioxythiophene):poly (styrenesulfonate) (PEDOT:PSS) which is favorably available as an aqueous dispersion and often utilized as hole injection layer in polymer electronic devices. PEDOT:PSS also has many functions in electronic devices to enhance the electrode performance by adjusting the work function of an electrode [8, 9], modifying the defects on ITO surface and for implication as a flexible anode [10]. Recently, some research groups have investigated film morphology and electrical properties of PEDOT:PSS by several techniques such as conductive atomic force microscopy (C-AFM) [11], micromolding in capillaries (MIMIC) [12], and nanoimprinting (soft-embossing) method [13]. Although the aforementioned techniques can produce micro/nano scale grating structures of the polymer surfaces, some of these techniques are adverse in some ways. For example, in C-AFM case, the conducting probe demands rather a long time to texture the surface features and causes decrease of local film conductivity owing to mass transport of PSS-rich regions to the surface under applied bias. The effective area is also limited by the inherent trait of tip size. As for the MIMIC process, it preferably creates edge thickening arising from a meniscus at the interface between the PDMS mold wall and the polymer solution. The very slow filling rate of small capillaries may hinder the possibility of MIMIC in many types of fabrication system. In addition, the nanoimprinting method requires a sophisticated and elaborate mold to duplicate and transfer grating patterns during direct contact with the polymer surface. Furthermore, the heating procedure results in unnecessary or additional annealing effect on the photoactive layer in organic electronic devices. In most conditions, however, conducting polymers have to be modified to work with these techniques.

In the present work, we demonstrate the implementation of the rubbing method in the fabrication of an organic-based bulk heterojunction solar cell. The rubbing procedure is the most widely used industrial technique for rapid, simple and inexpensive formation of alignment polymer film over large areas in LCDs (liquid crystal displays) [14]. As a result of previous reports and other papers [15, 16], it is well known that the director of nematic LC (liquid crystal) tends to assume an orientation parallel to the direction in which an adjacent solid surface has previously been rubbed. A crucial concept is that LC molecules could be uniformly oriented by the grooves (wavy surface) of the organic material layer which is caused in the rubbing action. In these studies, these grooves had periods in the range of micrometers to hundreds of nanometers, with relief depths between a few tens and a few hundreds of nanometers. The surface properties of different surface roughness induced by rubbing method were related to polymer structural, morphological and optical properties. Therefore, the employment of periodic structures as an efficient light-trapping plot was investigated for high performance OPV (organic photovoltaic) cells based on P3HT and PCBM bulk heterojunction. The nanoscale grooves of PEDOT:PSS layer were achieved by a lithography free method, so called rubbing process. With this configuration, the periodic grooves increase light absorption in consequence of scattering light occurring within the hole carrier transporting interface between the rubbed PEDOT:PSS and the photoactive layer. Moreover, the morphology of the rubbed PEDOT:PSS surface facilitates the hole carrier collection rate owing to the increased surface area of the interfaces. Most important of all, there are no further modification or treatment on the PEDOT:PSS solution, for example dilution and extra additives. The PCE of polymer solar cells inserted with a grooved PEDOT:PSS layer was enhanced by a simple and fast rubbing treatment. The related measurements and results of this rubbed buffer layer in BHJ solar cell devices suggest the feasibility of this renowned

rubbing method can be applicable to large scale fabrication of polymer based solar cells.

2. Experiments

Here we demonstrate an unprecedented approach, namely rubbing method, of using wavelength scale structure to increase the incident light absorption in organic photovoltaic cells. Fig. 1 shows the flow chart of the fabrication process. First, the ITO glass substrate was cleaned with detergent, acetone and isopropyl alcohol in an ultrasonic bath, before being dried under nitrogen flow. The PEDOT:PSS (Clevios P VP AI4083, H.C. Starck) was spin-coated (40 nm) on the ITO surface, followed by heating at 140 °C for 10 min. In general, the rubbing process is performed by contacting and moving a rotating cylinder (covered with a rubbing cloth) over a polymer-coated substrate at a constant velocity which is shown in Fig. 1a. The grooves (grating-like features) were produced on the PEDOT:PSS surface by the rubbing procedure. The rubbing treatment which is a physical activity was done using a machine whose drum was wrapped with a velvet cloth. Rubbing the surface scribes small grooves (or threads) on the PEDOT:PSS surface as presented in Fig. 1b. The grooves produced during rubbing process are grating-like structure with a periodicity of 500 nm. All the rubbing steps were performed in ambient conditions. The rubbed or un-rubbed PEDOT:PSS-coated substrates were prepared for the next step of active layer coating. Regioregular P3HT was prepared using the Grignard Metathesis approach [17], providing regiocontrol in each coupling step in the polymeric reaction. The regioregularity was characterized by 1H NMR to be greater than 96%. The mixtures of P3HT (15 mg·mL^{-1}) and PCBM (Nano-C, 12 mg·mL^{-1}) were dissolved in 1 mL of chlorobenzene. Meanwhile, those PEDOT:PSS-coated substrates were transferred into a nitrogen-filled glove box. Then the P3HT:PCBM blend was spin-coated on top of the PEDOT:PSS pre-coated ITO substrate (15 Ω·□$^{-1}$), and a P3HT:PCBM active layer of about 130 nm was formed. Subsequently, metallic cathodes of Ca (20 nm) and Al (100 nm) were deposited on top of the active layer by thermal evaporation at a pressure of approximately 10^{-6} Torr. The complete solar cell device is exhibited in Fig. 1c. The device area was 0.06 cm^2 which was defined through a shadow mask allowing the realization of four cells onto the same substrate. Devices to be annealed were placed on a digitally controlled hot plate at 150 °C for 10 min under N_2 atmosphere after the cathode was evaporated.

To study the performances of solar cells with or without rubbed PEDOT:PSS layer, current density-voltage (J-V) characteristics were measured using a programmable Keithley mode 2400 instrument. The solar simulator (Oriel 91160) consists of an Oriel xenon arc lamp with an AM 1.5G solar filter and the 100 mW·cm^{-2} intensity was calibrated with a mono-Si reference cell with a KG5 filter (PV Measurements, Inc.), which was calibrated by National Renewable Energy Laboratory (NREL), according to the procedure

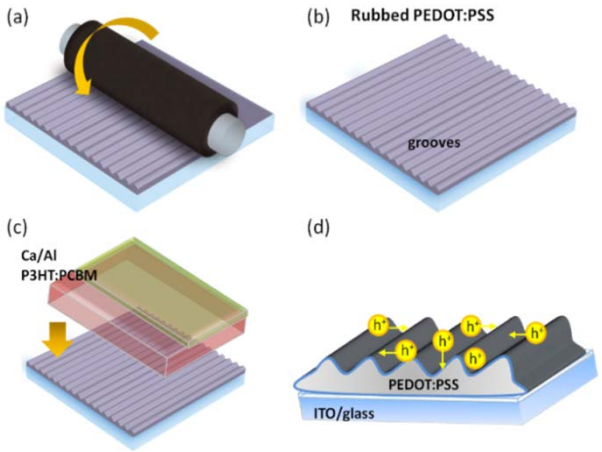

Fig. 1 Schematic representation of the flow chart of the rubbing process applied in the formation of nanoscale grooves on the PEDOT:PSS surface. (a) The PEDOT:PSS-coated film is rubbed by a rotating cylinder which is covered with velvet cloth. (b) The rubbed grooves produced during rubbing process is a wavy-like structure with a periodicity of 500 nm and around 10 nm deep. (c) The polymer solar cell device structure consists of ITO/rubbed PEDOT:PSS/P3HT:PCBM/Ca/Al. (d) Schematic diagram of a larger interface area made by the rubbing process and continuous hole carrier transporting pathways to the ITO electrode.

described elsewhere [18]. The mismatch factor was not considered here. The morphology of the rubbed PEDOT:PSS surface and the thickness of each layer were investigated using the atomic force microscope (AFM). The UV-vis absorption and photoluminescence spectra of the active layer were visualized with the aid of a UV-vis spectrometer (JASCO V-670) and Fluorolog Tau 3 (Jobin Yvon), respectively. The reflectance spectra of the active film were obtained by using a UV-vis-NIR spectrometer (JASCO ILN-725) with an integrating sphere. The IPCE (incident-photon-to-current conversion efficiency) spectra were recorded under illumination by a 450 W xenon lamp with a monochromator (TRIAX 180, JOBIN YVON), and the light intensity was calibrated using an OPHIR 2A-SH power meter. All reflectance, UV-vis, and PL samples were prepared by spin-coating the blend solution of P3HT and PCBM on the PEDOT:PSS/ITO substrates which include the rubbed and non-rubbed samples. To make hole-only devices, Ca/Al was replaced with higher work function Au as the top contact. A 100 nm thickness of Au layer was thermally evaporated on top of the active layer under a pressure of 4×10^{-6} Torr. In order to have reference measurements for the photovoltaic behavior, we classify these samples into the rubbed and the planar solar cell device, respectively.

3. Results and Discussion

To highlight the scientific and technological challenges for highly efficient organic solar cells, we discuss some parameters strongly depending on the morphology of rubbed PEDOT:PSS layer in organic BHJ solar cells which were compared with equivalent cells made by the conventional processing methods. In most rubbing cases, the polymer film is rubbed with another organic polymer material, also called “cloth” which is composed of the synthetic fibers having a variety of chemical structures. It is the nature of the rub material as well as the surface coating that determines the microscopic structure of the treated surface layer [19]. Reportedly the action of rubbing produces very high localized heating which results in melting of one of the polymer materials [20]. It means that the material with higher melting temperature causes melting of the material with lower melting point. Since the heating generated in the rubbing process is enough to melt the PEDOT:PSS film (T_m = 149 °C) locally [19-21]. In our case, the cloth via rubbing process accounts for the oriented grooves produced in PEDOT:PSS layer. The rubbing treatment leads to the nanoscale-groove structure on the surface of PEDOT:PSS layer. The RS (rubbing strength) is expressed by the following formula [22]:

$$RS = NM(2\pi rn/v\text{-}1) \quad (1)$$

where, N is the number of the repeated times for the rubbing (usually N = 1 in our work), M is the depth of the deformed fibers of the cloth due to the pressed contact (mm), n is the rotation rate of the drum (1,700/60 s^{-1}), v is the translating speed of the substrate (20.0 mm·s^{-1}), and r is the radius of the drum. The RS is given in mm unit. In this research the calculated RS is about 396 mm (M ~1 mm, r = 42 mm, n = 28.3 Hz, and v = 20.0 mm·s^{-1}).

The AFM images shown in Fig. 2 were captured in tapping mode, revealing the surface relief structure of the planar and the rubbed PEDOT:PSS films. In Fig. 2a the planar PEDOT:PSS layer shows flat surface while the rubbed PEDOT:PSS layer in Fig. 2b demonstrates that the orientation of grooves is uniformly aligned

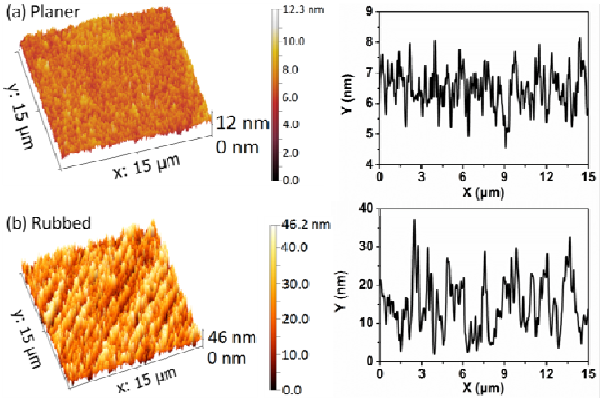

Fig. 2 The surface topography and height variation of (a) planer and (b) grooved PEDOT:PSS films prepared by the rubbing process. (AFM image dimensions: 15 μm × 15 μm).

along the rubbing direction. The profile of the rubbed structure shows that the periodicity of the wavy-like grooves is ~ 500 nm, and the depth of the feature is ~10 nm. Wavelength scale structures can modify the generation and propagation of light in materials [23]. In addition, small-scale corrugation enables large-area PEDOT:PSS/active layer interfaces, the surface roughness (mean roughness) of PEDOT:PSS layer increases from 0.80 nm to 7.63 nm after rubbing treatment. The interface area of the rubbed sample increases ~ 1.10% compared with the planar sample. The enhanced interface makes hole carriers transportation extensive as depicted in Fig. 1d. The expected effect of increased surface area is to reduce the distance which newly separated charge carriers will migrate through organic semiconductors before extraction from the device. Such structuring of the buffer layer would potentially increase the light absorbed within the active layer, since the optical path length is increased for light diffracted at angles other than normal to incident. By means of the rubbing process, polymorphism control of organic semiconductor films could greatly affect photovoltaic device performance. In contrast with photolithographic processes, the approach used in this study is a non-destructive and non-complex approach for patterning polymers. Furthermore, the use of rubbing process has several advantages such as a one-step process, feasible duplication and ease of fabrication.

To further characterize the thin film morphologies, we extracted the values of the hole mobility from the dark current density-voltage characteristics of the hole-only devices. We fabricated these devices using a high work-function material, gold (Au), as cathode to block the injection of electrons. The hole mobility was calculated precisely by fitting the dark J-V curves for single carrier devices using SCLC (space charge-limited current) model at low voltages, where the current is given by the equation [24]:

$$J = 9\varepsilon_0\varepsilon_\rho\mu V^2(8L)^{-3} \quad (2)$$

where, $\varepsilon_0\varepsilon_\rho$ is the permittivity of the polymer, μ is the carrier mobility, and L is the device thickness. From the dark J-V curves, the obtained hole mobility of the device with the planar PEDOT:PSS layer is (6.19 ± 0.13) × 10^{-5} $cm^2 \cdot V^{-1} \cdot s^{-1}$. On the other hand, for the devices treated with rubbed process, the hole mobility increases to (7.58 ± 0.37) × 10^{-5} $cm^2 \cdot V^{-1} \cdot s^{-1}$. The increased hole mobility observed upon rubbed PEDOT:PSS layer suggests that the rubbing process benefits to increase the interface area between PEDOT:PSS and the photoactive layer which facilitates hole carrier transportation. Since the electron mobility of PCBM is larger than the hole mobility of conjugated polymer, hole accumulation often occurs in the device and the photocurrent is space-charge limited, leading to a lower fill factor [25]. In our experiments, the hole mobility in the polymer increases by almost 22% so that the electron/hole transport becomes fairly balanced. As a result, the relatively high hole mobility of the rubbed PEDOT:PSS sample increases as a consequence of efficient hole collection via increased contact area, leading to a better device efficiency.

The photovoltaic performance of the P3HT:PCBM based organic photovoltaic cells inserted with planar and rubbed PEDOT:PSS films, under the AM 1.5 G illumination at an incident intensity of 100 $mW \cdot cm^{-2}$ is shown in Fig. 3. The planar device exhibits an open-circuit voltage (V_{oc}) of 0.59 V, a short-circuit

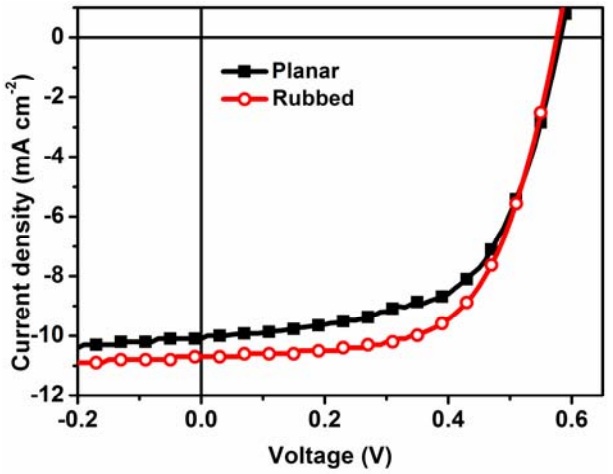

Fig. 3 J-V characteristics (AM 1.5 G, 100 $mW \cdot cm^{-2}$) of P3HT:PCBM based solar cells inserted with the planar and the rubbed PEDOT:PSS films.

current density (J_{sc}) of 10.05 ± 0.08 mA·cm^{-2}, a fill factor (F.F.) of 58.7% ± 0.4%, and a power conversion efficiency (PCE) of 3.45% ± 0.05%. As expected, the effect of rubbing treatment on PEDOT:PSS surface, we have achieved improved solar cell device performance with an increased J_{sc} of 10.70 ± 0.07 mA·cm^{-2}, a raised F.F. of 61.6% ± 0.1% and an enhanced PCE of 3.82 ± 0.03%. To determine the effect on the film internal resistance caused by grating morphology, R_s (device series resistances) and R_{sh} (shunt resistances) were derived from the slopes of the J-V curves. The R_s of the rubbed device is reduced by rubbing method (to values as low as 8.44 Ω·cm^2), which is consistent with the increased Jsc. Also, the rubbed device shows an increased R_{sh} (~ 0.55 kΩ·cm^2) which corresponds to less chance of charge recombination. Previous work has demonstrated that pentacene preferentially grows on an inclined plane (the hillside of a grain boundary) which was used to induce the bulk phase forming in the early stage of pentacene film growth [26, 27]. Herein, we speculate that the rubbed buffer layer is able to influence the formation of the P3HT bulk phase at small thickness (< 10 nm) on nanoscale undulated PEDOT:PSS surface and align the P3HT polymer chains. The detailed organic photovoltaic performance parameters of the P3HT:PCBM based solar cells with/without the aid of rubbing process are summarized in Table 1.

Photocurrent generation is mainly governed by three major factors: they are the number of absorbed photons; the numbers of carriers generated by the charge separation of excitons at the donor and acceptor interface and the charge-collection efficiency [28]. In order to characterize the optical performance of planar and rubbed PEDOT:PSS samples, the absorption spectra of P3HT:PCBM films on each sample were examined. Fig. 4 shows the absorption spectra of P3HT:PCBM films on the planar and rubbed PEDOT:PSS layer. There are three vibronic absorption shoulders at 525, 555 and 600 nm, respectively, in the visible region for the P3HT:PCBM blend films, which can be ascribed to the absorption of P3HT. The peak at 525 nm is the absorption of P3HT main chain, and the other two peaks in the longer wavelength are due to the interchain interactions in the ordered P3HT crystalline regions in the films [29]. Comparing two samples with the same active layer thickness, an obvious enhancement in absorption around 525 and 555 nm is observed in the sample with the rubbed PEDOT:PSS layer. The features of rubbed PEDOT:PSS layer can be used as subwavelength scattering elements to couple and trap freely propagating light into an active layer, by diffracting the light into the photon absorber [30]. The scattered light has longer pathways in the active layer and thus increases the possibility of photon absorption. This method could be regarded as a promising approach to improve light absorption without increasing photoactive-layer thickness. Moreover, the rubbed PEDOT:PSS surface shows higher reflectance relative to the planar sample (Fig. 5), which leads to more photons reflected from metal cathode reflected back to the active layer, results in more possibility of photon absorption. Irregularities in grooves will assist the rubbed device to make a broadband collection of photons in order to increase the photocurrent.

The photoluminescence spectra of devices with different PEDOT:PSS films were measured at an excitation wavelength of 550 nm and shown in Fig. 6. The photoluminescence intensity of the P3HT:PCBM film on the planar PEDOT:PSS layer exceeds that of the one on the rubbed surface although the latter has higher absorbance at the excitation wavelength. This finding supports the presence of the grooving structure can greatly increase the interfacial area between the

Table 1 The performance parameters of P3HT:PCBM based solar cells with/without the aid of rubbing process are summarized.

	V_{oc} (V)	J_{sc} (mA·cm^{-2})	F.F. (%)	PCE (%)	R_s (Ω·cm^2)	R_{sh} (kΩ·cm^2)
Planar	0.59	10.05	58.7	3.45	9.06	0.51
Rubbed	0.58	10.70	61.6	3.82	8.44	0.55

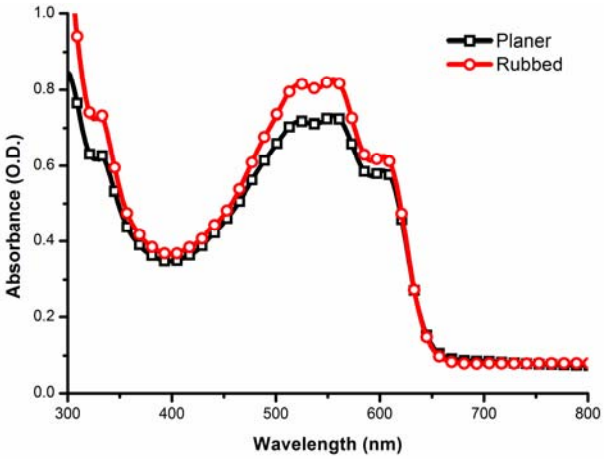

Fig. 4 UV-vis absorption spectra of the active films (P3HT:PCBM = 1:0.8) deposited on the planar and the rubbed PEDOT:PSS layers.

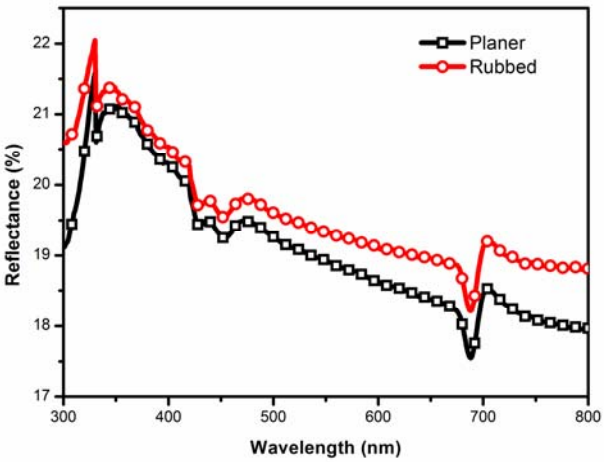

Fig. 5 Reflectance spectra of the planar and the rubbed PEDOT:PSS layers on glass substrates.

blend materials and the buffer layer and the efficiency of photoinduced carrier transfer. Besides, it has been shown that the amount of PCBM in active layer is richer than P3HT near the surface of PEDOT:PSS layer, which increases the possibility of electron/hole recombination when hole carriers transport toward buffer layer [31]. Therefore, the undulated surface of PEDOT:PSS layer, which can be viewed as a protrusion sticking out into the active layer, could further enhanced the interface between PEDOT:PSS and the P3HT-rich part in the active layer as Fig. 6b illustrated. As a result, controlling the surface morphology can facilitate extraction of holes as it will in some regions shorten the distance they have to travel to the electrode. The rubbing method induced performance improvement is attributed to the increased number of absorbed photons and promoting carrier transport behavior.

Consequently, as shown in Fig. 7, the device with the rubbed layer demonstrates higher IPCE throughout the visible range compared with the device without the rubbed layer. Because the integration of the product of the IPCE with the AM 1.5G solar spectrum is equal to J_{sc}, the higher J_{sc} (Fig. 3) of the device with rubbed layer is consistent with the higher IPCE values. All IPCE curves closely follow the absorption spectra of the P3HT:PCBM blend and maximum efficiency wavelength of the IPCE located at around 525 nm. Enhancement of PCE inherently coupled with enhanced

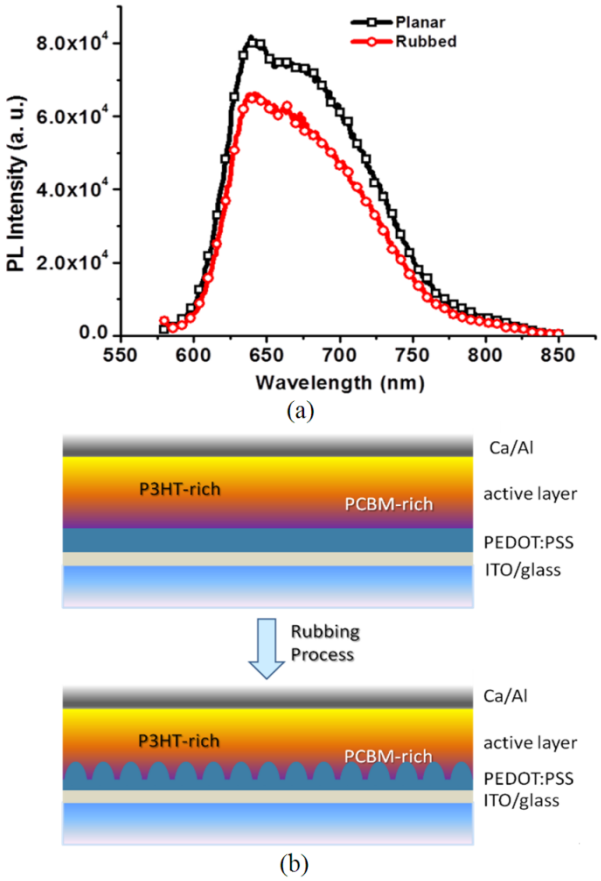

Fig. 6 (a) Photoluminescence spectra of the active films (P3HT:PCBM = 1:0.8) deposited on the planar and the rubbed PEDOT:PSS layers and (b) schematic diagram of the interface enhancement between PEDOT:PSS and the P3HT-rich part in the active layer.

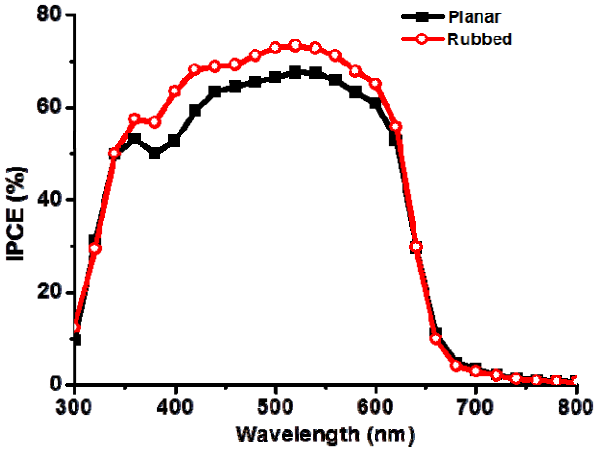

Fig. 7 IPCE spectra of P3HT:PCBM based solar cells inserted with the planar and the rubbed PEDOT:PSS films.

photon absorption for increased exciton generation and subsequent exciton dissociation efficiency gains to form free charge carriers. At maximum peak position the enhancement of IPCE is around 10%. Here, most of the increase in the cell efficiency is from the increased J_{sc} through the application of periodic structures rather than V_{oc}. It means that rubbed grooves induce more photogenerated charge carriers by stronger absorption of an active layer, resulting from the increase of optical path length and light trapping. IPCE and PCE of OPV cells with grooved buffer layers increase primarily due to enhanced J_{sc}, indicating the grooves created by the rubbing method cause further photon absorption in active layers and better hole transportation (charge carrier mobility) within the interface between PEDOT:PSS and the active layer. In addition, the size effect of grooves could be one of the factors for such results. Further studies by the authors are under progress and will be reported in due course.

4. Conclusions

We envisage that the grooved structure could readily be mass produced by the rubbing method, a technique that is very mature and successfully used for the manufacture of LCDs, has been unprecedentedly demonstrated for organic photovoltaic cells. In our work, the obtained PCE in the presence of a rubbed PEDOT:PSS layer is 3.82%, which is higher than the corresponding PCE 3.45% of the planar device. Moreover, the hole carrier mobility, optical absorbance, and excitons dissociation rate have been improved due to the resultant grooved morphology on the surface of PEDOT:PSS layer. This synergistic performance enhancement is believed to originate from the oriented interfaces that facilitate charge transport, moderate ordering of bulk heterojunction materials near the interfaces, and some light scattering to the photoactive layer from the nanoscale grooved surface. As this simple rubbing technique is inexpensive and suitable for roll-to-roll manufacturing over large areas, it may contribute to the goal of efficient solar energy conversion using organic polymers and molecules. From this standpoint, the rubbing technique is a potential technology for large scale fabrication of polymer based solar cells.

Acknowledgments

This work was supported by the National Science Council and Ministry of Education of the Republic of China. The authors would like to thank Dr. Chin-Wei Liang for his assistance and helpful discussions.

References

[1] C.J. Brabec, N.S. Sariciftci, J.C. Hummelen, Plastic solar cells, Adv. Funct. Mater. 11 (2001) 15-26.

[2] G. Li, V. Shrotriya, J. Huang, Y. Yao, T. Moriarty, K. Emery, et al., High-efficiency solution processable polymer photovoltaic cells by self-organization of polymer blends, Nat. Mater. 4 (2005) 864-868.

[3] W.L. Ma, C.Y. Yang, X. Gong, K.H. Lee, A.J. Heeger, Thermally stable, efficient polymer solar cells with nanoscale control of the interpenetrating network morphology, Adv. Funct. Mater. 15 (2005) 1617-1622.

[4] Y. Kim, S. Cook, S.M. Tuladhar, S.A. Choulis, J. Nelson, J.R. Durrant, et al., A strong regioregularity effect in self-organizing conjugated polymer films and high-efficiency polythiophene: Fullerene solar cells, Nat. Mater. 5 (2006)197-203.

[5] G. Zhao, Y. He, Y. Li, 6.5% efficiency of polymer solar cells based on poly(3-hexylthiophene) and indene-C60 bisadduct by device optimization, Adv. Mater. 22 (2010) 4355-4358.

[6] B. Crone, A. Dodabalapur, Y.Y. Lin, R.W. Filas, Z. Bao, A. LaDuca, et al., Large-scale complementary integrated

circuits based on organic transistors, Nature 403 (2000) 521-523.

[7] L.B. Groenendaal, F. Jonas, D. Freitag, H. Pielartzik, J.R. Reynolds, Poly(3,4-ethylenedioxythiophene) and its derivatives: Past, present, and future, Adv. Mater. 12 (2000) 481-494.

[8] T.M. Brown, J.S. Kim, R.H. Friend, F. Cacialli, R. Daik, W.J. Feast, Built-in field electroabsorption spectroscopy of polymer light-emitting diodes incorporating a doped poly(3,4-ethylene dioxythiophene) hole injection layer, Appl. Phys. Lett. 75 (12) (1999) 1679-1681.

[9] V. Shrotriya, G. Li, Y. Yao, C.W. Chu, Y. Yang, Transition metal oxides as the buffer layer for polymer photovoltaic cells, Appl, Phys. Lett. 88 (2006) 073508-073510.

[10] D. Li, L.J. Guo, Micron-scale organic thin film transistors with conducting polymer electrodes patterned by polymer inking and stamping, Appl. Phys. Lett. 88 (2006) 063513-063515.

[11] X.D. Dang, M. Dante, T.Q. Nguyen, Morphology and conductivity modification of pol(3,4-ethylenedioxythiophene):poly(styrene sulfonate) films induced by conductive atomic force microscopy measurements, Appl. Phys. Lett. 93 (2008) 241911-241913.

[12] F. Zhang, T. Nyberg, O. Inganäs, Conducting polymer nanowires and nanodots made with soft lithography, Nano Lett. 2 (2002) 1373-1377.

[13] Y. Yang, K. Lee, K. Mielczarek, W. Hu, A. Zakhidov, Nanoimprint of dehydrated PEDOT:PSS for organic photovoltaics, Nanotechnology 22 (2011) 485301-485305.

[14] P.G. de Gennes, J. Prost, The Physics of Liquid Crystals, Oxford University Press, New York, 1993, pp. 34-35.

[15] M. Nishikawa, N. Bessho, T. Natsui, Y. Ohta, N. Yoshida, D.S. Seo, et al., A model of the unidirectional alignment accompanying the pretilt angle of a nematic liquid crystal (NLC),5CB, oriented on rubbed organic-solvent-soluble polyimide film, Mol. Cryst. Liq. Cryst. 275 (1996) 15-25.

[16] D.S. Seo, O.I. Toshio, H. Matsuda, T.R. Isogami, K.I. Muroi, Y. Yabe, et al., Surface morphology of the rubbed polyimide and polystyrene films and their liquid crystal aligning capability, Mol. Cryst. Liq. Cryst. 231 (1993) 95-106.

[17] R.S. Loewe, S.M. Khersonsky, R.D. McCullough, A simple method to prepare head-to-tail coupled, regioregular poly(3-alkylthiophenes) using grignard metathesis, Adv. Mater. 11 (1999) 250-253.

[18] V. Shrotriya, G. Li, Y. Yao, T. Moriarty, K. Emery, Y. Yang, Accurate measurement and characterization of organic solar cells, Adv. Funct. Mater. 16 (2006) 2016-2023.

[19] J.A. Castellano, Surface anchoring of liquid crystal molecules on various substrate, Mol. Cryst. Liq. Cryst. 94 (1983) 33-41.

[20] A. Adamson, Physical Chemistry of Surfaces, John Wiley & Sons, 3rd ed., New York, 1976, p. 246.

[21] M.D. Irwin, D.A. Roberson, R.I. Olivas, R.B. Wicker, E. MacDonald, Conductive polymer-coated threads as electrical interconnects in e-textiles, Fiber Polym. 12 (2011) 904-910.

[22] D.S. Seo, S. Kobayashi, M. Nishikawa, Study of the pretilt angle for 5CB on rubbed polyimide films containing trifluoromethyl moiety and analysis of the surface atomic concentration of F/C(%) with an electron spectroscope for chemical analysis, Appl. Phys. Lett. 61 (1992) 2392-2394.

[23] B.J. Matterson, J.M. Lupton, A.F. Safonov, M.G. Salt, W.L. Barnes, I.D. Samuel, Increased efficiency and controlled light output from a microstructured light-emitting diode, Adv. Mater.13 (2001) 123-127.

[24] V. Shrotriya, Y. Yao, G. Li, Y. Yang, Effect of self-organization in polymer/fullerene bulk heterojunctions on solar cell performance, Appl. Phys. Lett. 89 (2006) 063505-063507.

[25] C. Melzer, E.J. Koop, V.D. Mihailetchi, P.W.M. Blom, Hole transport in poly(phenylene vinylene)/ methanofullerene bulk-heterojunction solar cells, Adv. Funct. Mater. 14 (2004) 865-870.

[26] H.L. Cheng, Y.S. Mai, W.Y. Chou, L.R. Chang, X.W. Liang, Thickness-dependent structural evolutions and growth models in relation to carrier transport property in polycrystalline pentacene thin films, Adv. Funct. Mater. 17 (2007) 3639-3649.

[27] M.H. Chang, W.Y. Chou, Y.C. Lee, H.L. Cheng, H.Y. Chung, Polymorphic transformation induced by nanoimprinted technology in pentacene-film early-stage growth, Appl. Phys. Lett. 97 (2010) 183301-183303.

[28] G.Yu, J. Gao, J.C. Hummelen, F. Wudl, A.J. Heeger, Polymer photovoltaic cells: Enhanced efficiency via a network of internal donor-acceptor heterojunctions, Science 270 (1995) 1789-1791.

[29] P.J. Brown, D.S. Thomas, A. Kohler, J.S. Wilson, J.S. Kim, C.M. Ramsdale, et al., Effect of interchain interactions on the absorption and emission of poly(3-hexylthiophene), Phys. Rev. B 67 (2003) 064203-064218.

[30] H.A. Atwater, A. Polman, Plasmonics for improved photovoltaic devices, Nat. Mater. 9 (2010) 205-213.

[31] M. Campoy-Quiles, T. Ferenczi, T. Agostinelli, P.G. Etchegoin, Y. Kim, T.D. Anthopoulos, et al., Morphology evolution via self-organization and lateral and vertical diffusion in polymer: Fullerene solar cell blends, Nature Mater. 7 (2008) 158-164.